The RNA-binding protein DDX1 promotes primary microRNA maturation and inhibits ovarian tumor progression

Cecil Han, Yunhua Liu, Guohui Wan, Hyun Jin Choi, Luqing Zhao, Cristina Ivan, Xiaoming He, Anil K. Sood, Xinna Zhang, Xiongbin Lu

Inventory of Supplemental Information

Figure S1

A

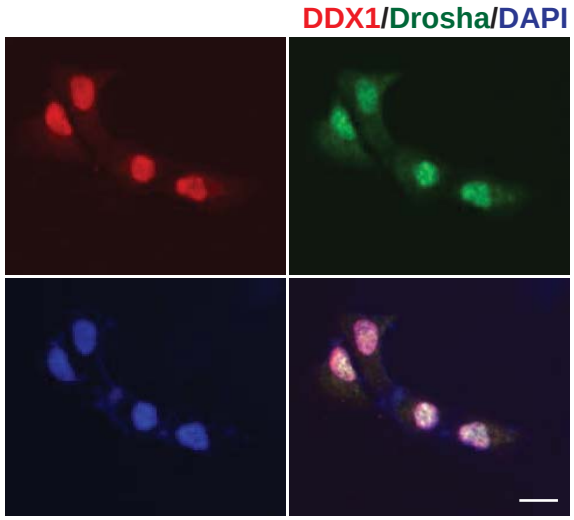
DDX1/Drosha/DAPI

B

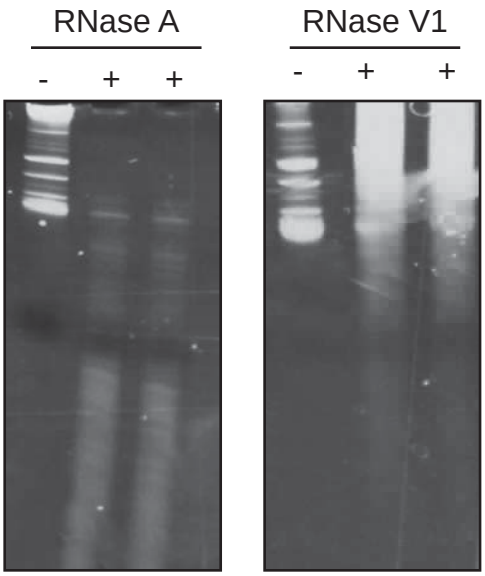
RNase A
RNase V1
- + +
- + +

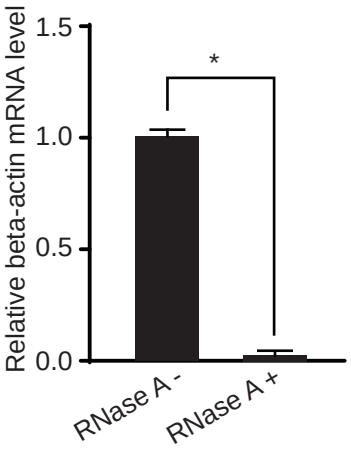
Relative beta-actin mRNA level
1.5
1.0
0.5
0.0
*
RNase A -
RNase A +

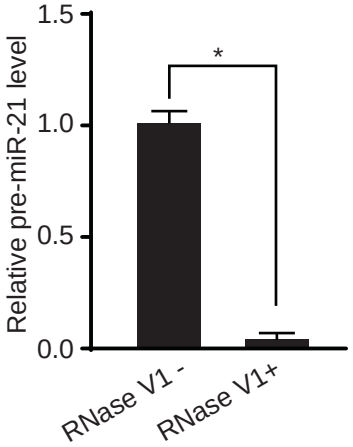
Relative pre-miR-21 level
1.5
1.0
0.5
0.0
*
RNase V1 -
RNase V1+

Figure S2

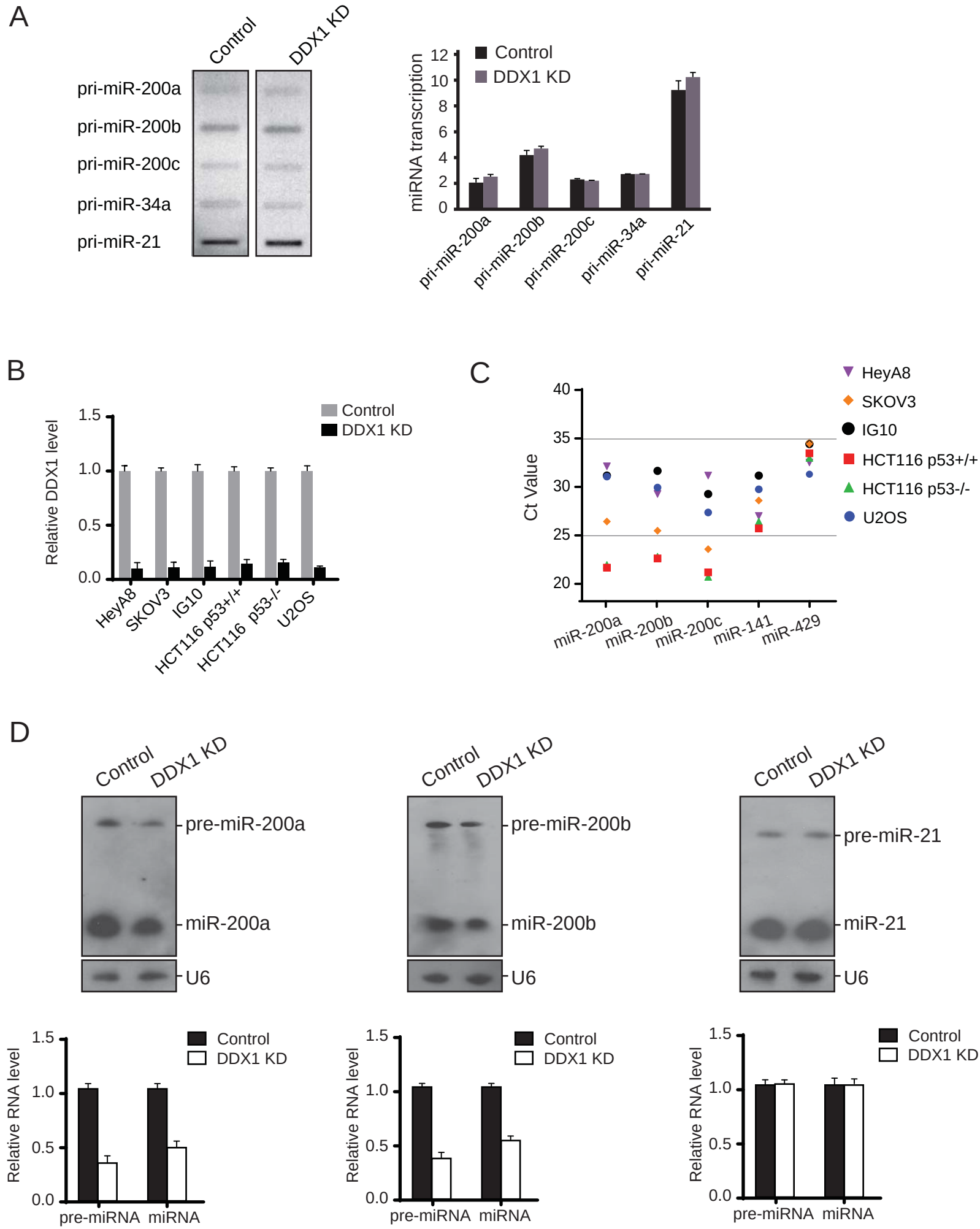
A
Control
DDX1 KD
pri-miR-200a
pri-miR-200b
pri-miR-200c
pri-miR-34a
pri-miR-21
miRNA transcription
Control
DDX1 KD
B
Relative DDX1 level
Control
DDX1 KD
HeyA8
SKOV3
IG10
HCT116 p53+/+
HCT116 p53-/-
U2OS
C
Ct Value
HeyA8
SKOV3
IG10
HCT116 p53+/+
HCT116 p53-/-
U2OS
miR-200a
miR-200b
miR-200c
miR-141
miR-429
D
Control
DDX1 KD
pre-miR-200a
miR-200a
U6
pre-miR-200b
miR-200b
pre-miR-21
miR-21
Relative RNA level
pre-miRNA
miRNA

Figure S3

A

DDX1-shRNA1 : CAGATGGTCTTTGTTGTCA
DDX1-shRNA2: AGATGGTCTTTGTTGTCAA

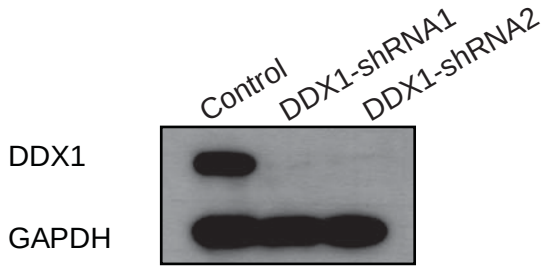

B

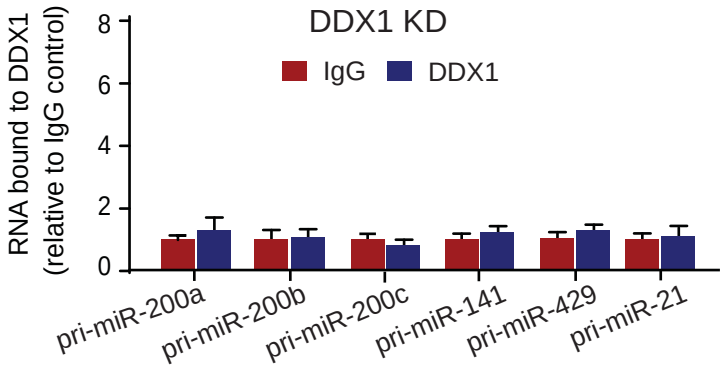

C

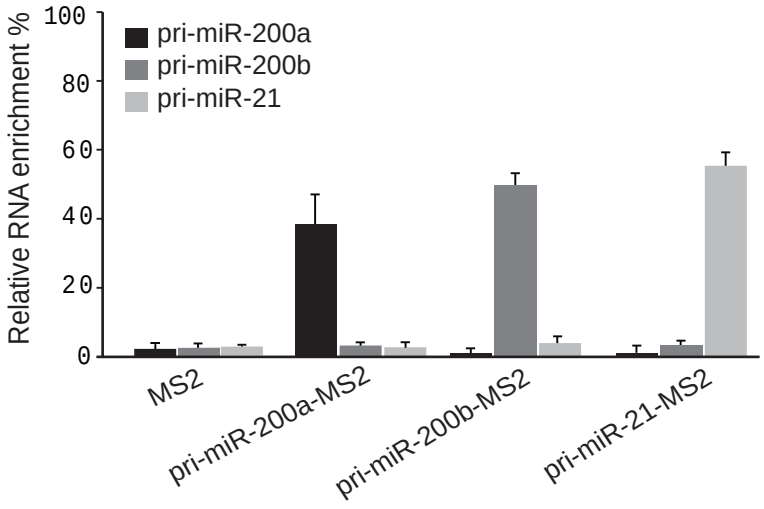

D

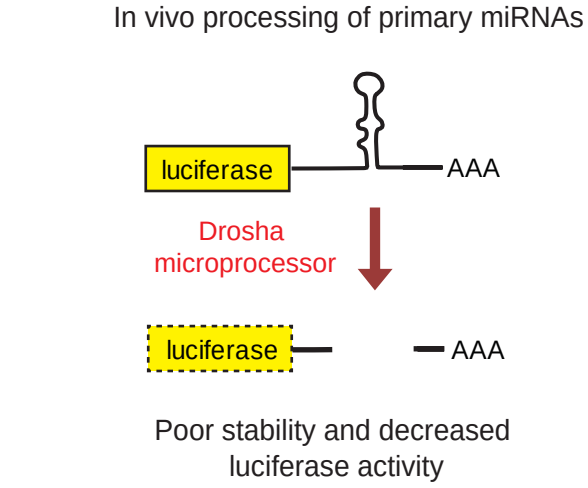

E

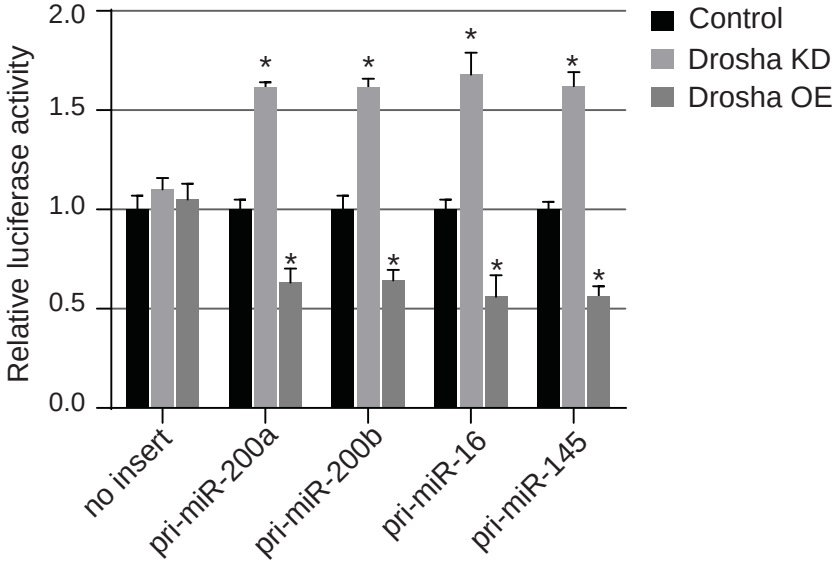

Figure S4

A

pri-miR-200b (WT)

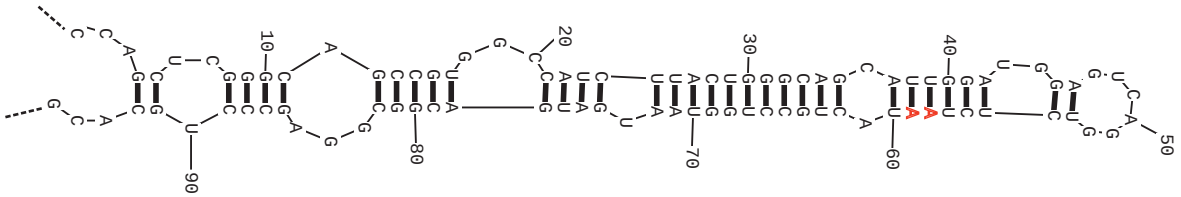

pri-miR-200b (mt)

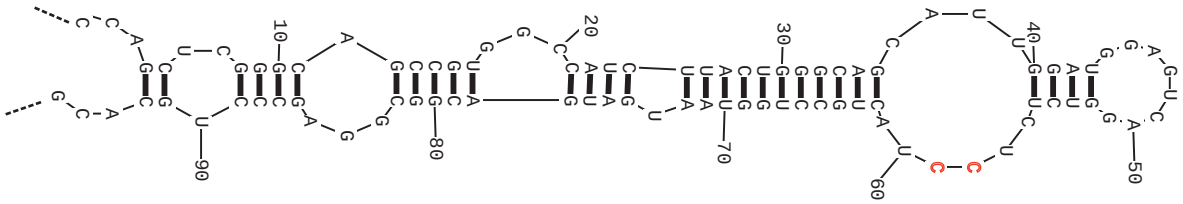

pri-miR-200a (WT)

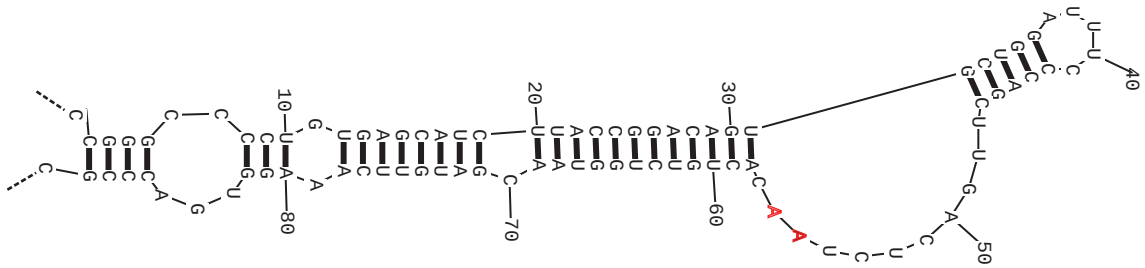

pri-miR-200a (mt)

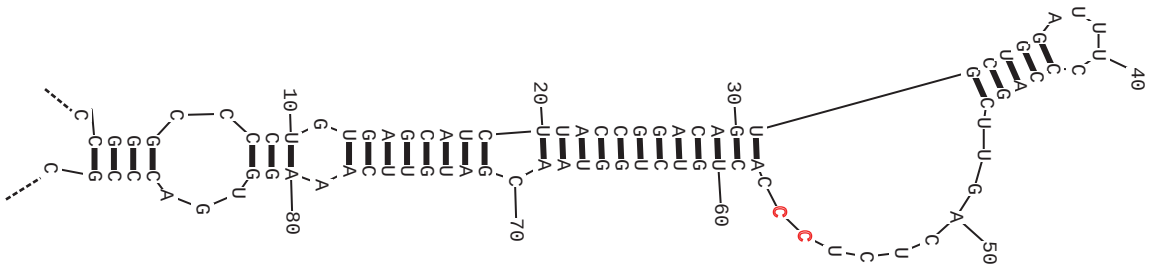

B

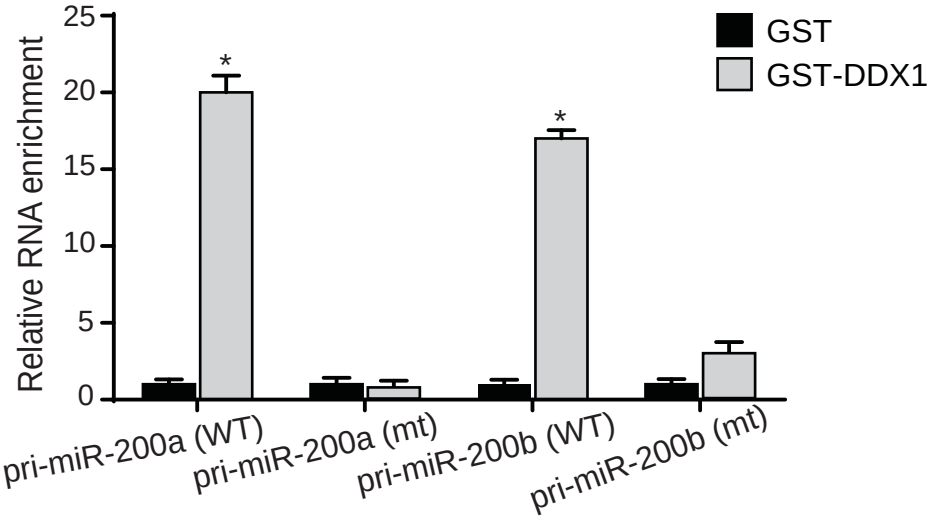

Figure S5

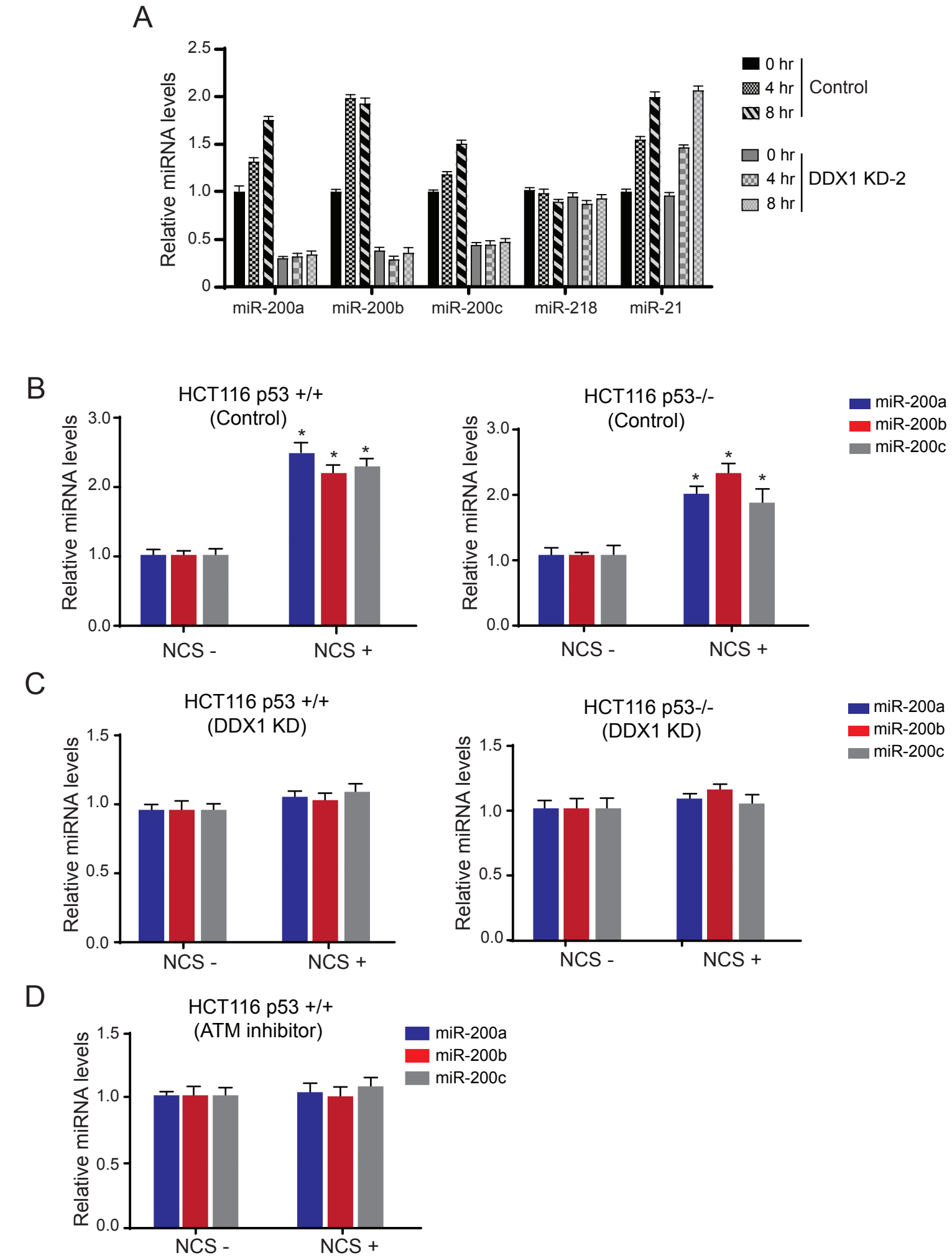
A
Relative miRNA levels
2.5
2.0
1.5
1.0
0.5
0
0 hr
4 hr
8 hr
Control
0 hr
4 hr
8 hr
DDX1 KD-2
miR-200a
miR-200b
miR-200c
miR-218
miR-21
B
HCT116 p53 +/+
(Control)
HCT116 p53-/-
(Control)
Relative miRNA levels
3.0
2.0
1.0
0.0
NCS -
NCS +
miR-200a
miR-200b
miR-200c
C
HCT116 p53 +/+
(DDX1 KD)
HCT116 p53-/-
(DDX1 KD)
Relative miRNA levels
1.5
1.0
0.5
0.0
NCS -
NCS +
miR-200a
miR-200b
miR-200c
D
HCT116 p53 +/+
(ATM inhibitor)
Relative miRNA levels
1.5
1.0
0.5
0.0
NCS -
NCS +
miR-200a
miR-200b
miR-200c

Figure S6

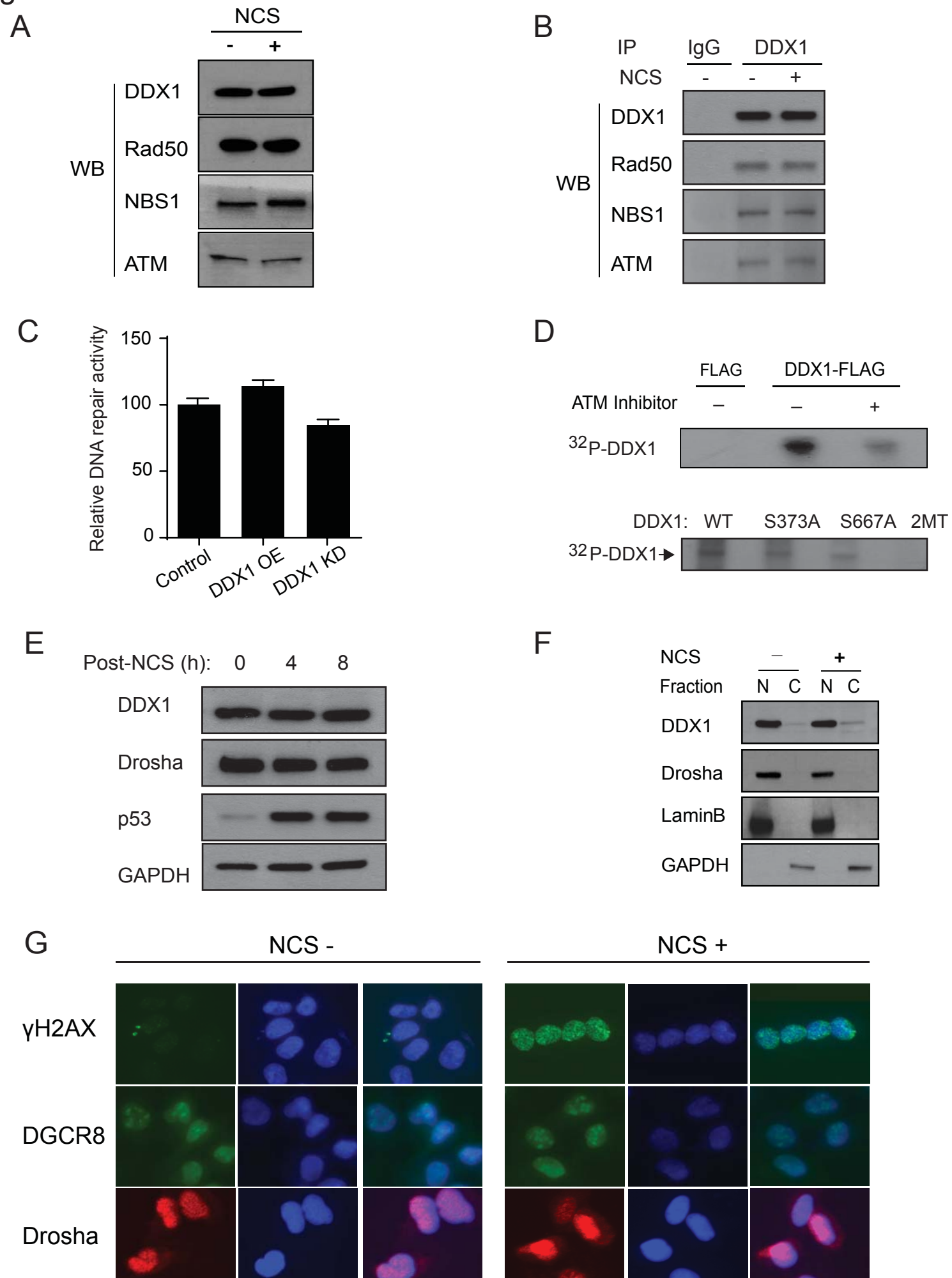
A
NCS
- +
WB
DDX1
Rad50
NBS1
ATM
B
IP IgG DDX1
NCS - - +
WB
DDX1
Rad50
NBS1
ATM
C
Relative DNA repair activity
150
100
50
0
Control
DDX1 OE
DDX1 KD
D
FLAG DDX1-FLAG
ATM Inhibitor – – +
32P-DDX1
DDX1: WT S373A S667A 2MT
32P-DDX1
E
Post-NCS (h): 0 4 8
DDX1
Drosha
p53
GAPDH
F
NCS – +
Fraction N C N C
DDX1
Drosha
LaminB
GAPDH
G
NCS -
NCS +
γH2AX
DGCR8
Drosha

Figure S7

A

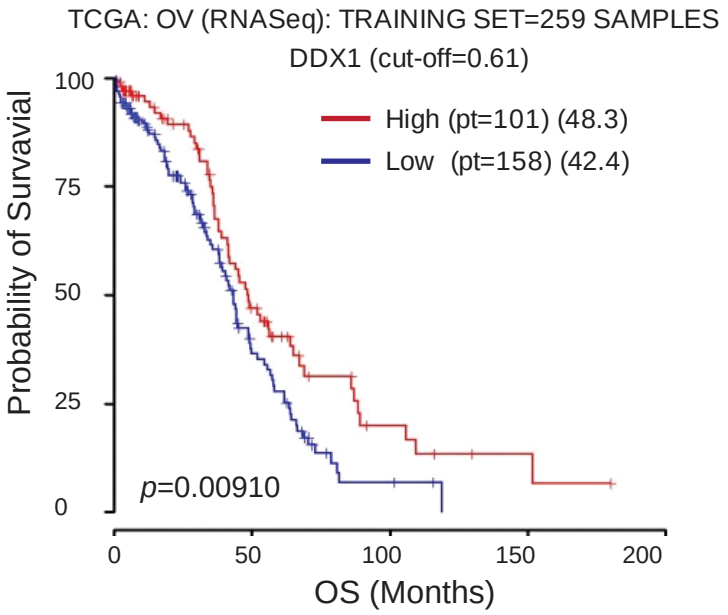

B

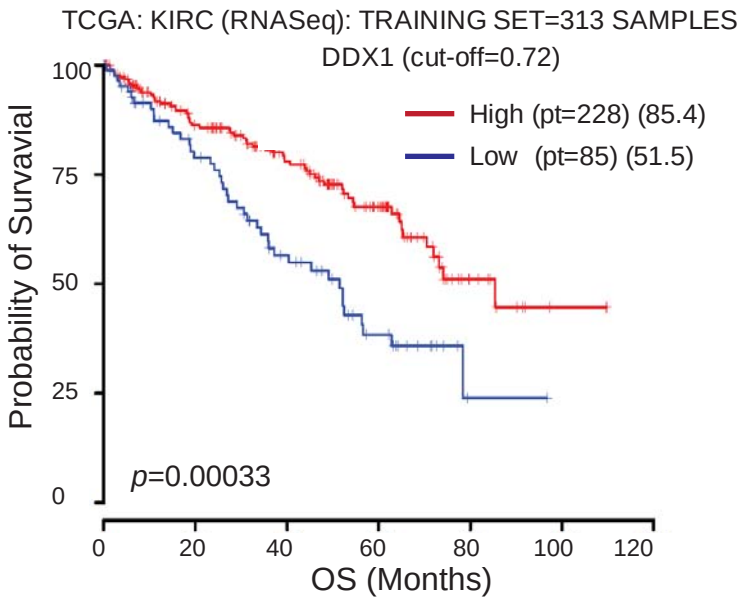

C

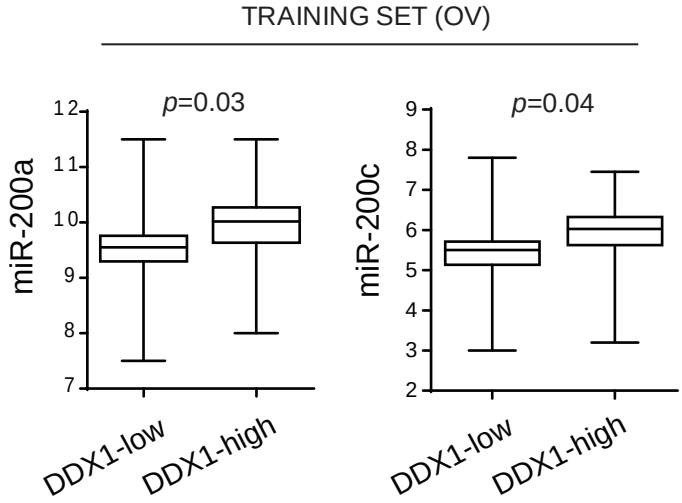

D

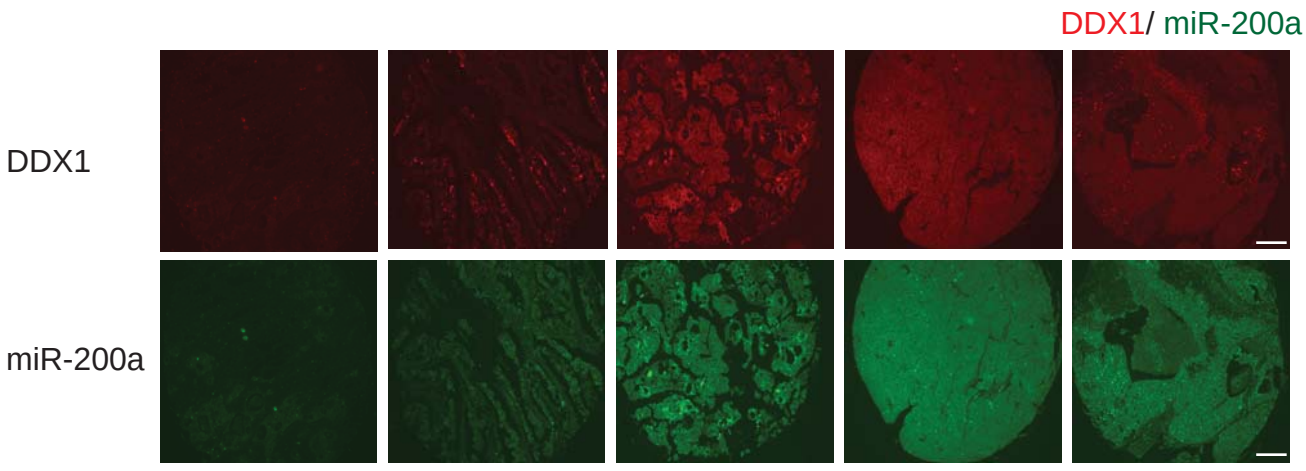

SUPPLEMENTAL FIGURE LEGENDS

Figure S1 (related to Figure 1). DDX1 interacts with the Drosha microprocessor. (**A**) Co-localization of DDX1 and Drosha in human U2OS cells. Scale bar: 10μm. (**B**) RNase activity was determined by incubating total RNA with 0.1 unit of RNase A or RNase V1 for 30 min. Integrity of RNA was observed by gel separation and ethidium bromide staining (two left panels). RNA degradation was evaluated by reduced levels of β-actin mRNA (single-stranded RNA) or pre-miR-21 (double-stranded RNA). * $p < 0.05$.

Figure S2 (related to Figure 2). Posttranscriptional regulation of the DDX1-dependent miRNA expression. (**A**) Transcription of the DDX1-dependent miRNA genes in control and DDX1-knockdown cells in nuclear run-on assays. Pri-miR-34a and pri-miR-21 were used as DDX1-independent miRNA controls. Quantification of transcription activities were shown on the right. (**B**) Efficiency of DDX1 knockdown in various cell lines. GAPDH levels were used for normalization. (**C**) CT (cycle threshold) values of DDX1-dependent miRNAs in qPCR assays. (**D**) Effect of DDX1 on miRNA processing. Northern blotting was performed to determine the levels of pre-miRNAs and mature miRNAs in total RNAs purified from control and DDX1-knockdown cells. U6 RNA was used as a loading control. Band intensity was quantified with Image J.

Figure S3 (related to Figure 3). DDX1 physically binds pri-miR-200s and promotes their processing. (**A**) Knockdown efficiency of two DDX1 shRNAs. (**B**) To test the specificity of DDX1 RIP assay, levels of pri-miRNAs were measured in the DDX1 immunoprecipitates of DDX1-knockdown cells. Control IgG immunoprecipitates were used as negative controls. No significant differences were observed for pri-miRNA levels in the control or DDX1-knockdown

immunoprecipitates. (**C**) Immunoprecipitation of MS2-pri-miR-200a, MS2-pri-miR-200b and MS2-pri-miR-21 in MS2-TRAP assays. Pri-miRNA levels were measured by RT-qPCR. (**D**) Schematic diagram for in-vivo pri-miRNA processing assay. (**E**) In-vivo pri-miRNA processing activity is dependent on Drosha. Firefly luciferase signals were normalized by internal control Renilla luciferase readings and are shown as fold changes in comparison with luciferase control vector without pri-miRNA insert. Error bars represents the mean ± SD, * $p < 0.05$.

Figure S4 (related to Figure 3). DDX1-binding requirements in pri-miR-200s. (**A**) Predicted structures of pri-miR-200a and pri-miR-200b. WT (wildtype) and mt (mutant) forms of pri-miR-200a/b are shown. Two A residues in or near the loops of the pre-miRNAs are conserved in most of the DDX1-dependent miRNAs (Table S1). (**B**) Mutating the AA di-nucleotides to CC in pri-miR-200a/b abolished their interaction with DDX1. * $p < 0.05$.

Figure S5 (related to Figure 4). DNA damage-induced miR-200 expression is independent of p53. (**A**) Levels of miR-200a/b/c were induced after NCS (500 ng/ml) treatment in control U2OS cells, but not in the DDX1-knockdown U2OS cells using DDX1 shRNA-2. miR-218 and miR-21 were used as DDX1-independent controls. (**B**) Levels of miR-200a/b/c in HCT116 p53+/+ and HCT116 p53-/- cells treated with or without NCS (500 ng/ml, 4 h) (* $p < 0.05$). (**C**) Levels of miR-200a/b/c in the DDX1-knockdown HCT116 p53+/+ and HCT116 p53-/- cells treated with or without NCS (500 ng/ml, 4 h). (**D**) Levels of miR-200a/b/c in HCT116 p53+/+ cells treated with NCS (500 ng/ml) and ATM inhibitor (10 μM of CGK733).

Figure S6 (related to Figure 5). Interaction between DDX1 and the Drosha complex is unchanged after DNA damage. (**A**) Protein levels of DDX1, Rad50, NBS1 and ATM are unchanged after NCS treatment (500 ng/ml, 4 h). (**B**) Interactions of DDX1 with Rad50, NBS1

and ATM are unchanged after NCS treatment. (**C**) Homologous recombination DNA repair activity is only minimally affected by DDX1. (**D**) DDX1 is phosphorylated in vivo. DDX1-overexpressing HEK293T cells were treated with or without ATM inhibitor (10 μM, CGK733) and phosphorylated proteins were labelled with ^{32}P-ATP. In vivo phosphorylation of wildtype and phosphorylation-mutant DDX1 (single or double sites) was shown at the bottom. (**E**) Protein levels of DDX1 and Drosha are unchanged throughout 0-8 h post-NCS treatment. p53 and GAPDH were used as positive and negative controls for DNA damage signalling, respectively. (**F**) Subcellular distributions of Drosha and DDX1 are unchanged after DNA damage (500 ng/ml NCS, 4 h). Lamin B and GAPDH were used as biomarkers for nuclear and cytoplasmic proteins, respectively. (**G**) Localization of Drosha and DGCR8 was unchanged after DNA damage (500 ng/ml NCS, 4 h). No distinct foci were observed for either Drosha or DGCR8 following DNA damaging treatment.

Figure S7 (related to Figure 7). DDX1 levels are associated with clinical outcome of cancer patients. (**A**) Kaplan-Meyer plots for overall survival of patients with ovarian serous adenocarcinoma in the training cohort (n = 259). (**B**) Kaplan-Meyer plots for overall survival of patients with kidney renal clear cell carcinoma (n = 313). (**C**) Relative expression levels of miR-200a (p = 0.03) and miR-200c (p = 0.04) in the DDX1-low and -high groups from the training cohort of ovarian serous adenocarcinomas. (**D**) Representative images for DDX1 and miR-200a levels in human ovarian tumor tissue microarray (Biomax, BC110118,). DDX1 levels are correlated with miR-200a levels. Scale bar: 200 μm.

Table S1. Alignment of DDX1 dependent pre-miRNAs using Clustal W.

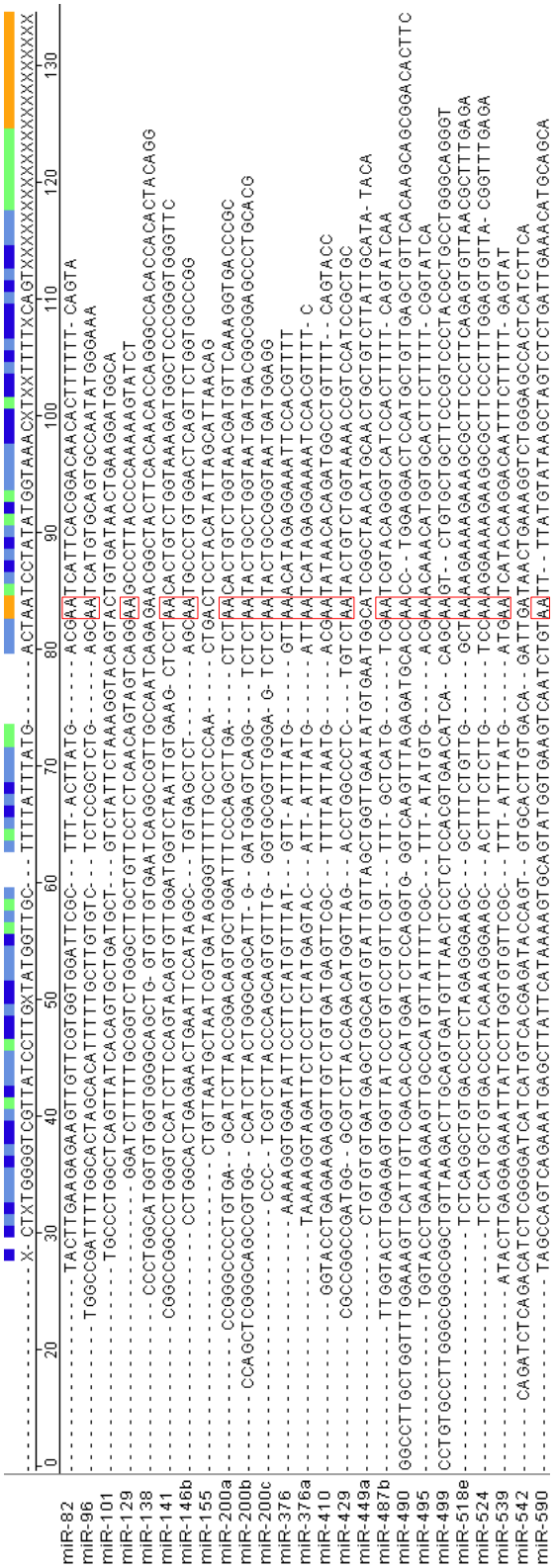

Table S2. Primers for mature miRNAs in qRT-PCR assays were obtained from Exiqon: U6 RNA control (#201510), miR-200a (#204707), miR-200b (#204650), miR-200c (#204482), miR-141 (#204504), miR-429 (#205068), miR-21 (#204230), miR-10a (#204778). Other primers specific for qRT-PCR are listed below.

pri-miR-21- forward	TTTTGTTTTGCTTGGGAGGA
pri-miR-21- reverse	AGCAGACAGTCAGGCAGGAT
pri-miR-10a- forward	CGGAAAGTAGGAGAACTGGA
pri-miR-10a- reverse	CAGAAAAATACTACATATAC
pri-miR-200a- forward	GATGCAAGGGTCAGAAGGGC
pri-miR-200a- reverse	GAGCCATCTGGCCCGGACG
pri-miR-200b- forward	CTGGCGGGACCCCACGTC
pri-miR-200b- reverse	TGCCTCGGTGGTGTCCCCG
pri-miR-200c- forward	CCTGGGCCTGAAGCTGCCT
pri-miR-200c- reverse	GGCGATGGATGTTGCTGAC
pri-miR-141- forward	GAGCGCGCACCGTAGTTCT
pri-miR-141- reverse	CCTGAAGGTTACTGCCGAG
pri-miR-429- forward	CGGAGGCCACCCACACCA
pri-miR-429- reverse	GCGGATGGACGGTTTTAC
pre-miR-10a-forward	CTGTCTGTCTTCTGTA
pre-miR-10a-reverse	GAGCGGAGTGTTTAT
pre-miR-21-forward	ATGTTGACTGTTGAATCTCATGG
pre-miR-21-reverse	TGTCAGACAGCCCATCGAC
pre-miR-200a-forward	TGTGAGCATCTTACCGGACA
pre-miR-200a-reverse	GGGTCACCTTTGAACATCGT
pre-miR-200b-forward	ACCCAGCTCGGGCAGCCGT
pre-miR-200b-reverse	TCTAGATGCGTGCAGGGCT
pre-miR-200c-forward	GAAGCTGCCTGACCCAAG
pre-miR-200c-reverse	CAGGGATCTGCAGCTTTTC
pre-miR-141-forward	GGCCGGCCCTGGGTCCATCT
pre-miR-141-reverse	CCACCCGGGAGCCATCTTTA
GAPDH-forward	AGCCACATCGCTCAGACAC
GAPDH-reverse	GCCCAATACGACCAAATCC
Human DDX1-forward	TTGATGGGAAAGTTACCTACGG
Human DDX1-reverse	CAAGATGCAGGAAAGATGTCTG
Mouse DDX1-forward	AATGAAATGCAGCTACTTTCCG
Mouse DDX1-reverse	CTGTCTACATGACGTCAGAAGG
Human Drosha-forward	TGAAACACTATGATGACCACAG
Human Drosha-reverse	GATAAACCGTAACTCCTTCCAG